A Within-subject Comparison of Common Neuroimaging Protocols on MAGNETOM Prisma^{fit} and MAGNETOM Trio Scanners

Ross W. Mair[1, 2]; Stephanie McMains[1]

[1] Center for Brain Science, Harvard University, Cambridge, MA, USA
[2] Athinoula A. Martinos Center for Biomedical Imaging, Massachusetts General Hospital, Charlestown, MA, USA

Introduction

The Center for Brain Science – Neuroimaging Facility (CBS) at Harvard University is a key imaging resource for a wide array of university psychology department and medical school faculty in the Boston area. Started with the installation of a MAGNETOM Trio (Siemens Healthcare, Erlangen, Germany) in 2008, the center achieves a funded average usage by researchers of ~2000 hours per year with an approximately 1000 additional hours per year of use for maintenance, development, and educational purposes. As such, the scanner is used consistently and at near-capacity by an active and diverse group of scientists from Harvard and from other institutions, including Harvard teaching hospitals, in the Boston community.

The vast majority of this MRI data is task-based or resting-state functional MRI employing T2*-weighted echo-planar imaging, or blood-oxygen level dependent (BOLD) techniques. Sessions also include a T1-weighted high-resolution structural or anatomical scan for co-registration to the BOLD images, and sometimes for brain morphometry. Many researchers also supplement their sessions with a short diffusion-weighted MRI scan. While most user-groups are eager to embrace new imaging technology and techniques when there is an appropriate benefit to the quality of their neuroimaging data, a key factor to ensuring quality data over studies that may run over periods stretching from 2 months to 2 years

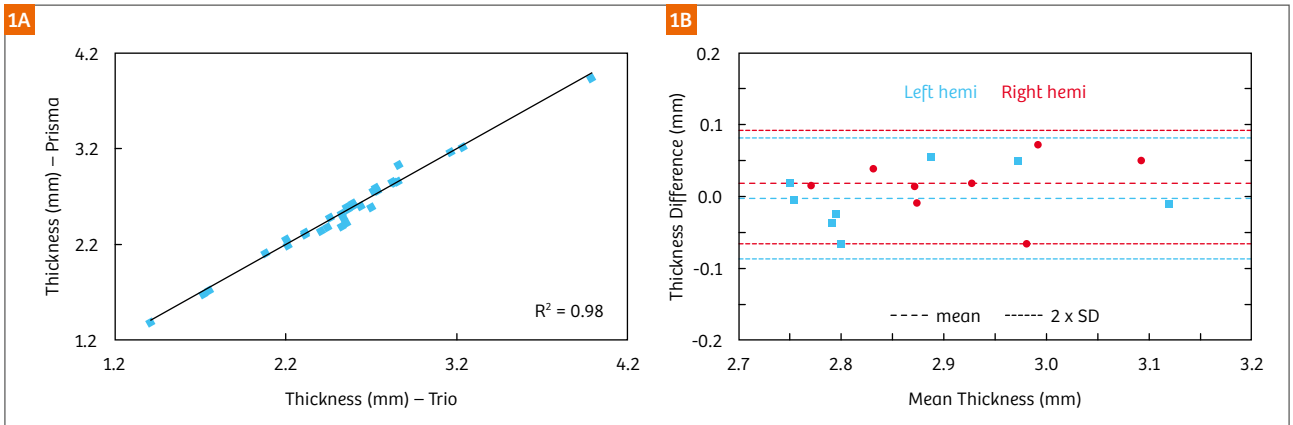

Figure 1:
(1A) Example correlation of cortical thickness of all 33 cortical regions of the Desikan-Killiany atlas from a single subject from T1-weighted images acquired on the MAGNETOM Trio and the MAGNETOM Prisma^{fit}. **(1B)** Example Bland-Altman difference plot of cortical thickness in the temporal lobes for 8 subjects from T1-weighted images acquired on the MAGNETOM Trio and the MAGNETOM Prisma^{fit}.

is stability and consistency of scanner performance, and continuity in image acquisition protocols and the resultant MRI data itself. At CBS, we have placed a very high priority on maintaining a stable and consistent scanning environment. As a result, when major imaging advances and hardware or software upgrades arrive, there are equal parts anticipation and trepidation for many of our user groups.

We upgraded the MAGNETOM Trio to the MAGNETOM Prisma^{fit} in the summer of 2015. The Prisma^{fit} represented a significant upgrade in performance capability over the Trio. The MAGNETOM Prisma platform included a major advance in gradient strength (80 mT/m, up from 45 mT/m), new highly-parallel array receive coils for the head, a digital RF transmit/receive architecture, and a much faster reconstruction computer. While the new gradient coil was expected to offer significant improvements in diffusion experiments, any change to the gradient system has the potential to bias brain morphometry data if there were changes in gradient linearity and performance. We believed the digital RF chain had the potential to significantly improve BOLD imaging with improved RF fidelity and a reduction in spurious noise pick-up, however it was unclear whether such benefits would hold up in the human head with its attendant physiological noise effects. In addition, as Simultaneous Multi-Slice imaging techniques were beginning to be adopted, the improved reconstruction system was seen as a key component that would allow routine use of this technique for high-temporal resolution BOLD imaging with real-time image reconstruction, rather than suffering often intolerable reconstruction lags, as was the case on the Trio.

To quantify the impacts and improvements offered by such a significant system upgrade, we scanned 8 subjects using a variety of anatomical, functional and diffusion protocols commonly employed at the time on the Trio platform, and then repeated the same scans with the same protocols on the Prisma^{fit} after the upgrade process. In addition, we devoted effort to assessing where the new hardware would permit improvements to temporal and spatial resolution in conventional BOLD imaging, both immediately after the hardware upgrade, and again following the software upgrade from *syngo* MR D13D to E11C in late 2016.

Methods

8 subjects were scanned on the 3T MAGNETOM Trio in July 2015. The same 8 subjects were scanned a second time on the MAGNETOM Prisma^{fit} in October 2015, after the scanner conversion. The relevant 32-channel head coil was used on each system. The scans included a 1.0 mm resolution multi-echo MPRAGE [1] anatomical scan acquired with FreeSurfer-recommended parameters (6:03 min, TR/TI = 2530/1100 ms, matrix 256 x 256 x 176, resolution = 1 x 1 x 1 mm (no partial fourier), parallel imaging acceleration (GRAPPA) = 2, pre-scan normalize enabled). Two resting state BOLD scans of 8-min duration were acquired, one with 3 mm resolution and TR = 3 s, the other with 2 mm nominal resolution, slice-acceleration [2, 3] (SMS) of 8 and TR = 750 ms. Additionally, a third BOLD scan employing a protocol commonly used for task studies at the time was acquired: 2 mm nominal resolution, SMS 3 and TR = 2 s. Two diffusion MRI protocols were employed, both with nominal 2 mm resolution: no SMS, 30 *b* directions, $b = 1000$ mm^2/s; and SMS 2, 64 *b* directions, $b = 1000$ mm^2/s. On the Prisma^{fit}, the diffusion protocols were reproduced exactly as implemented on the Trio, and then repeated utilizing the monopolar diffusion encoding scheme available in *syngo* MR D13 and E11, the performance gradient mode allowed by the Prisma^{fit} gradient set, and then optimizing the echo spacing and minimizing TE and TR. No changes were made to spatial resolution, number of *b* directions or *b* values, although it is widely expected such advances will become commonly employed on Prisma^{fit} system and similar scanners.

Anatomical images were analyzed using a FreeSurfer [4] processing stream. They were first corrected for gradient non-linearities according to the different scanner gradient coil parameters, after which the pairs of scans from each subject were aligned using the FreeSurfer robust registration tool [5]. FreeSurfer v.5.3 was used to perform an automated parcellation of the cortex, subcortical and white matter structures. The 33 cortical regions of the Desikan-Killiany atlas [6] were combined into five principal cortical lobes for simpler analysis [7]. Correlation and Bland-Altman difference plots were made for the thickness and volume of each principal cortical lobe determined from each scan, and for the volume of key sub-cortical structures. Surface-based plots were made to show regions of thickness difference and significance of difference. Diffusion scans were analyzed from raw DWI images and ADC and FA maps generated by the scanner software at the scanner console. In addition, diffusion scans were post-processed with a detailed stream that included gradient non-linearity correction, motion correction/realignment, eddy-current distortion correction, and registration to the anatomical space of the T1-weighted image. This alignment enabled the ADC and FA to be probed in the parcellated corpus callosum only, while the whole brain and white-matter-only masked images were analyzed for stability. BOLD scans were analyzed by assessing tSNR for each voxel, and averaged over the whole brain, after motion correction and detrending. Functional-connectivity

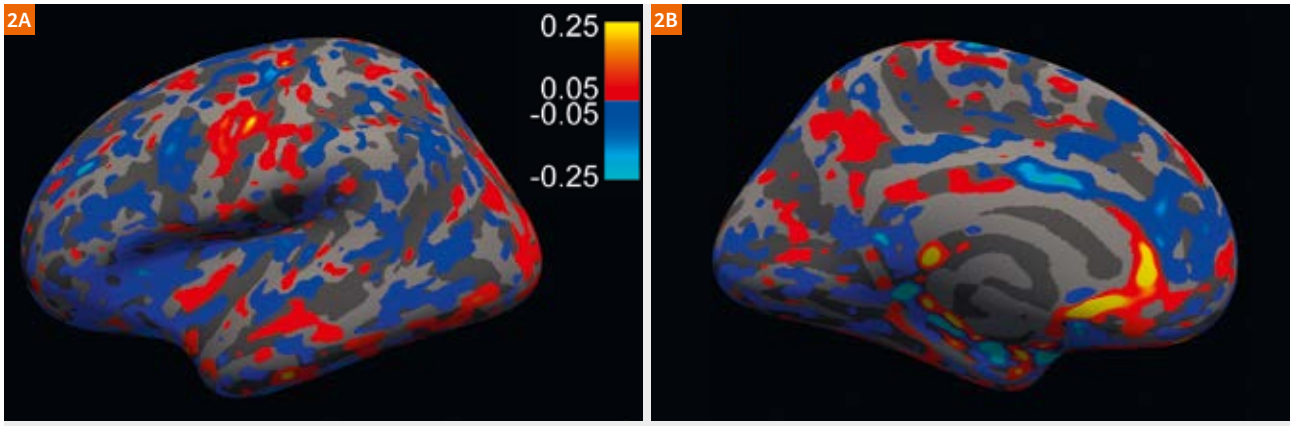

Figure 2:
Surface plots of average cortical thickness difference for pairs of T1-weighted images acquired on the MAGNETOM Trio and the MAGNETOM Prisma^{fit}. Thickness differences are threshold at ± 50–250 µm, color bars are in mm. The left hemisphere is shown – results are similar for the right hemisphere.

analysis was performed on the two resting-state BOLD scans with a seed-based correlation procedure using correlations between major network seeds [8].

Results/discussion – anatomical scans

The anatomical scans from each subject, acquired on the MAGNETOM Trio and on the MAGNETOM Prisma^{fit} appeared visually very similar. The offline gradient non-linearity correction modified the appearance of the neck/spine region on scans acquired on the Trio, but the brain and skull appeared unaffected. On the Prisma^{fit}, in addition to modification of neck/spine region, a slight extension to the crown of the skull and the parietal cortex just below it could be observed for some subjects following gradient non-linearity correction. Therefore, for comparison of brain morphometric data, gradient non-linearity correction was performed on the anatomical scans from each scanner, prior to robust registration of the pairs of scans to an unbiased base-space, after which the standard FreeSurfer processing stream was performed.

Figure 1A shows an example correlation plot for the thickness of all 33 cortical regions of the Desikan-Killiany atlas, from a single subject, as determined from images acquired on the Trio and on the Prisma^{fit}. Similar correlation plots were obtained for gray matter volume for the 33 cortical regions, and for the volumes of sub-cortical/white matter structures. Correlation Coefficients (R^2) were routinely ~0.95–1.00 for all subjects, and were especially high for the sub-cortical/white matter structure volumes. However, while intuitively simple, correlation plots can hide systematic biases, and so a Bland-Altman difference analysis was also performed. Figure 1B shows an example Bland-Altman difference plot, plotting the difference of the measured average cortical thickness of the temporal lobes for all eight subjects, when scanned on the Trio and on the Prisma^{fit}. The average thickness value was obtained from aggregating the relevant cortical regions from the Desikan-Killiany atlas for each subject [7]. The mean difference for both the left and right hemispheres was close to zero, with a standard-deviation inside ± 0.1 mm. Similar plots were obtained for the other principal cortical lobes, with differences always considerably less than ± 50 µm. Such differences are on the order of those seen for test-re-test scans on the same scanner on the same day [9]. For the sub-cortical/white matter structures, a wider range of differences were observed – up to ± 5%, but again were respectable compared to prior studies of variation between head coils or repeated measures on different days [10].

Figure 2 shows inflated-surface plots of cortical thickness difference for groups of scans on the Trio and on the Prisma^{fit}. Cortical thickness difference was determined using all 33 cortical regions of the Desikan-Killiany atlas for each scan, with each subject registered to FreeSurfer average-space, so differences can be analyzed on a single surface. Thickness differences are thresholded at ± 50 µm – the vast majority of difference observed is either below 50 µm (masked out), or between 50 and 100 µm. Only the inner surface of the temporal lobe and a spot in the central gyrus shows values higher. However, a t-test determined that none of the thickness differences are statistically relevant ($p > 0.01$).

In combination, the results from Figures 1 and 2 indicate that, with careful control for gradient non-linearity and

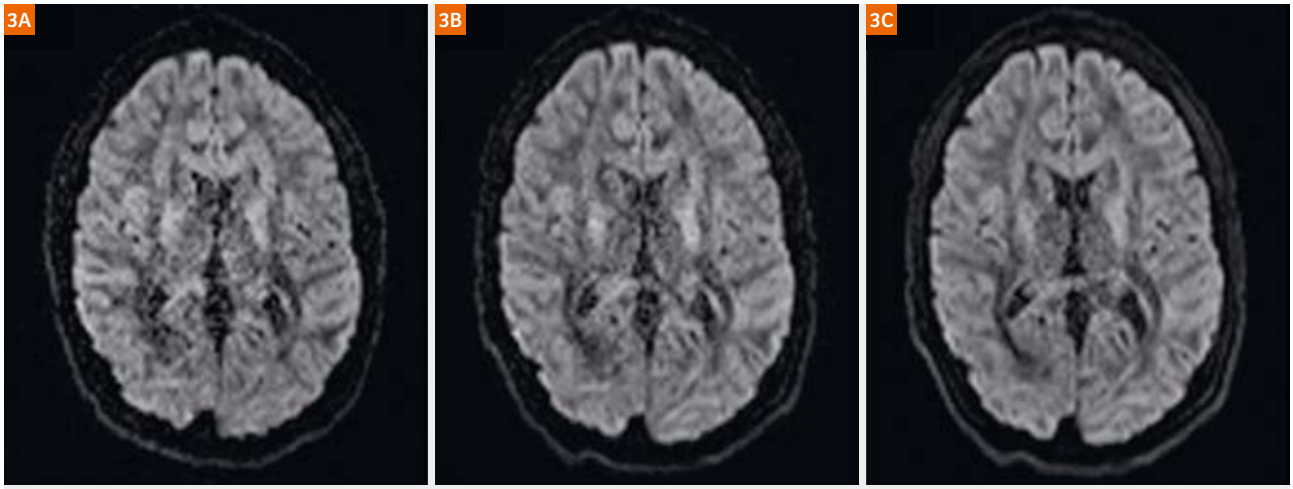

MAGNETOM Trio

MAGNETOM Trio protocol on MAGNETOM Prisma^{fit}

MAGNETOM Prisma^{fit} optimized

Figure 3:
Representative DWI images, as displayed at the scanner console, from the same subject acquired on the MAGNETOM Trio and the MAGNETOM Prisma^{fit}. A 2 mm isotropic, SMS = 2, 64-direction, *b* = 1000 s/mm^2 DTI protocol was used. **(3A)** Image from the Trio. **(3B)** Image from the Prisma^{fit} when the Trio protocol was implemented. **(3C)** Image from the Prisma^{fit} after optimizing echo-spacing, bandwidth, and TE as permitted by the Prisma^{fit} hardware.

robust registration, brain morphometric data should not be biased by scanner whether a Trio or Prisma^{fit} is used, or when the former is upgraded to the latter.

Results/discussion – diffusion scans

For the diffusion scans, the protocols used on the Trio were implemented exactly on the Prisma^{fit} without modification, to check for between-scanner variation, being cognizant of reducing bias for ongoing studies that straddled the upgrade period. Using "fast" gradient mode on the Sequence/Part 2 tab restricts the Prisma^{fit} gradient to the maximum strength and slew-rates employed on the Trio. These scans are referred to as "Trio protocol on Prisma", which we hoped would show insignificant variation from the scan on the Trio. The scans were then repeated employing the hardware and software advances of the Prisma^{fit}, principally the use of the monopolar diffusion encoding scheme which significantly reduces TE; the performance gradient mode allowed by the Prisma^{fit} gradient set allowing stronger gradient strengths with shorter gradient durations; and then optimizing the echo spacing and minimizing TE and TR as a result of the above changes. These scans are referred to as "Prisma optimized", although no changes were made to the spatial resolution, number of *b* directions or *b* values, as is likely for diffusion protocols truly optimized for the Prisma^{fit}.

Figure 3 shows a single slice from a diffusion-weighted image on the Trio, and the two corresponding scans on the Prisma^{fit}, all acquired with the 64-direction / SMS = 2 protocol. The reduction in TE, from 90 to 57 ms in the "Prisma optimized" protocol, results in a noticeable improvement in SNR in the DWI. The same impact is seen in the color-coded FA maps as generated by the scanner software without offline processing, which are shown in Figure 4. Again, the "Prisma optimized" protocol results in a noticeable improvement in SNR in the FA map. For the three marked ROI's shown in the images, which were chosen to comprise regions of highly uniform fiber orientation and density, an average reduction in the standard-deviation of FA in the three ROIs in the "Prisma optimized" image was found to be ~25%. For the same three ROI's, the average ADC standard-deviation fell by ~40% with the "Prisma optimized" protocol, but were otherwise similar for the Trio and the "Trio protocol on Prisma" scan.

To more carefully quantify the effect of the SNR increase and improved signal stability with the "Prisma optimized" protocol, the diffusion scans were also processed offline using a conventional processing stream including alignment to the T1-weighted image native space before recalculation of the ADC and FA images. The resultant ADC and FA images were then masked by the corpus callosum as derived from the FreeSurfer-processed T1-weighted image for each subject. Figure 5 shows the average of the standard-deviation of ADC and FA within the corpus callosum for the 8 subjects, using the two

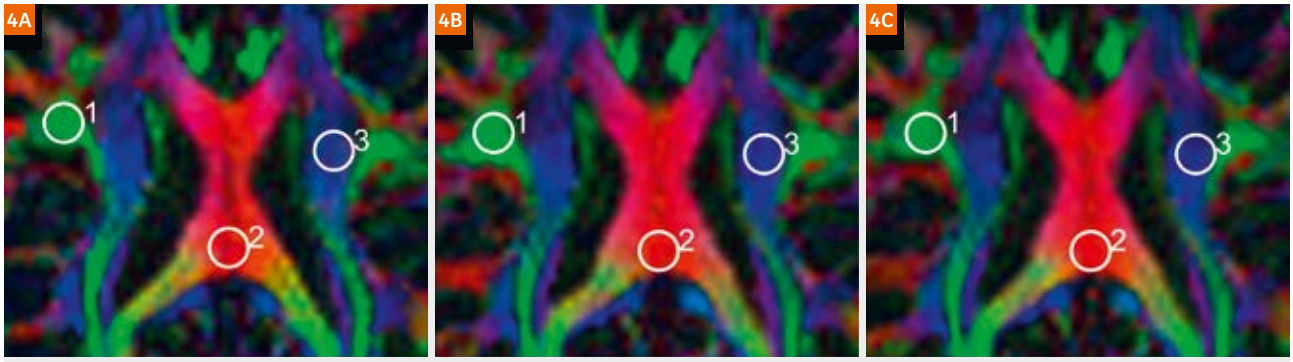

MAGNETOM Trio

MAGNETOM Trio protocol on MAGNETOM Prisma^{fit}

MAGNETOM Prisma^{fit} optimized

Figure 4:
A portion of the scanner-generated Color-FA maps from the same subject acquired on the MAGNETOM Trio and the MAGNETOM Prisma^{fit}. The same protocol from Figure 3 was used. **(4A)** FA image from the Trio. **(4B)** FA image from the Prisma^{fit} using the Trio protocol without modification. **(4C)** FA image from the Prisma^{fit} after optimizing as permitted by the Prisma^{fit} hardware. In the three ROIs shown, the ADC std-dev is ~40% lower and the FA std-dev is ~25% lower when the Prisma^{fit}-optimized protocol was used with this subject.

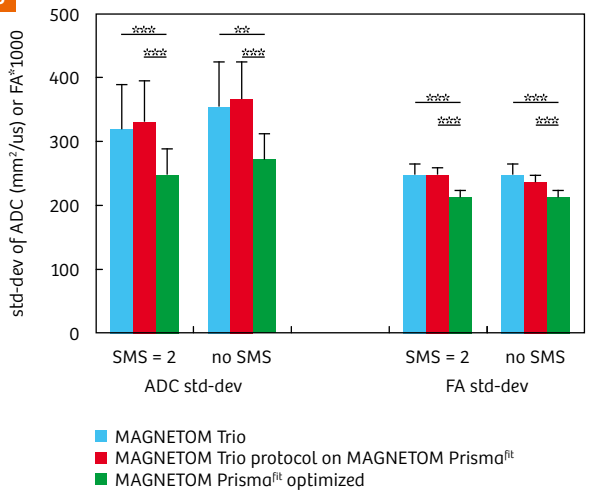

Figure 5:
Standard-deviation of the values of ADC and FA in the segmented corpus callosum, after detailed offline processing, for the three different scan procedures described in Figures 3 and 4 on the MAGNETOM Trio and MAGNETOM Prisma^{fit}, averaged over 8 subjects. Here, data from the SMS = 2 / 64-direction and the no SMS / 30-direction DTI protocols are shown.

acquisition protocols (SMS 2 / 64 directions, and no SMS / 30 directions) on the Trio, and for the "Trio protocol on Prisma" and "Prisma optimized" scans on the Prisma^{fit}. Noticeable reductions are seen in both the ADC and FA standard-deviations for the "Prisma optimized" scans for both protocols (all $p < 0.001$, except, "Trio protocol on Prisma" versus "Prisma optimized", $p < 0.01$); while the "Trio protocol on Prisma" and the original scan on the Trio essentially give indistinguishable results ($p > 0.05$).

Signal stability was also assessed from the repeated $b = 0$ images in each diffusion scan, in the same way it would be done for BOLD scans – dividing the mean image (after realignment) by the standard-deviation, to give a "time-series SNR" or tSNR image. This was done with 5 $b = 0$ images from each scan for the no SMS / 30 direction protocol, and 10 $b = 0$ images for the SMS 2 / 64 direction protocol. In each case, the metric was calculated on the whole brain after brain extraction, and on an image masked to show only the segmented white matter from the FreeSurfer-processed T1-weighted image for each subject. As shown in Figure 6, the "Prisma optimized" scans for both protocols exhibited improvements in tSNR of ~30–40% compared to the "Trio protocol on Prisma" and the original scan on the Trio (all $p < 0.001$), while the "Trio protocol on Prisma" and the original scan on the Trio were similar ($p > 0.05$).

These results show that the new, high-performance gradient coil that is the heart of the Prisma indeed delivers the expected boost of SNR to MRI diffusion scans, when the acquisition protocols are optimized to take full use of the new gradient strength and slew rate. The reduction in TE of ~30–40% for a commonly employed acquisition protocol can yield similar increases in diffusion-scan signal stability, and reduce the uncertainties in derived diffusion metrics by similar amounts. Of course, these new gradient capabilities are also being used to bring more advanced diffusion acquisition protocols into the mainstream, employing higher, and multiple, b values, and more diffusion directions; to improve fiber-tracking definition in areas where fibers cross. The multi-site Human Connectome Projects on Aging and Development, and the Adolescent Brain Cognitive Development (ABCD)

6

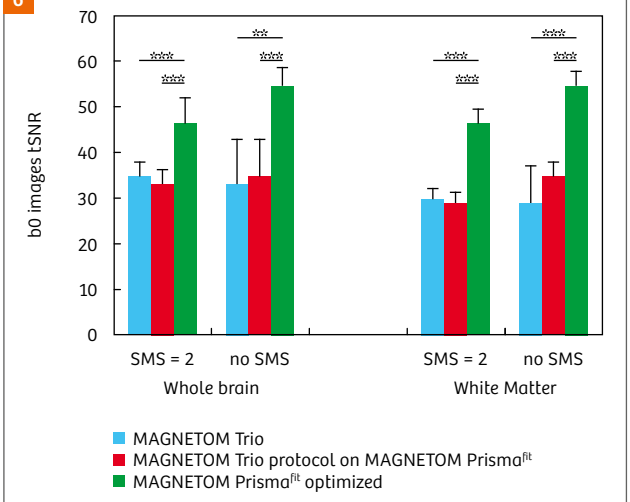

Figure 6:
DTI signal stability from repeated *b* = 0 images (labeled "tSNR"), averaged over 8 subjects, in the whole brain and in masked white matter, for the three different scan procedures described in Figures 3 and 4 on the MAGNETOM Trio and MAGNETOM Prisma^{fit}. The SMS = 2 / 64-direction protocol acquired 10 *b* = 0 images, and the no SMS / 30-direction protocol acquired 5 *b* = 0 images.

7

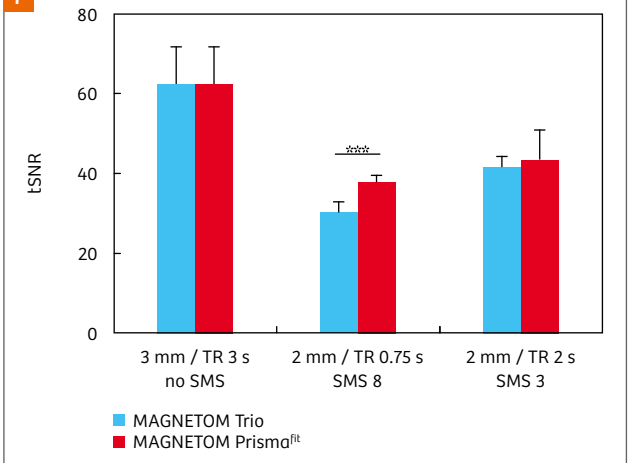

Figure 7:
Average whole-brain tSNR values measured in BOLD scans acquired on the MAGNETOM Trio and the MAGNETOM Prisma^{fit}.

study, both in the US, are both employing *b* values up to 3000 s/mm^2 with 100–200 *b*-vectors for routine use in studies that will scan thousands of subjects. Alternatively, for those wishing to replicate the diffusion protocol and data quality for studies ongoing from Trio scanners, the identical implementation of a protocol, with the gradient mode restricted to "Fast" mode, should give equivalent data on the Prisma.

Results/discussion – functional scans

Although Siemens Healthcare had not promised improvement to the quality and stability of EPI-BOLD scanning, we had initial hopes that some of the other hardware improvements, such as the all-optical transmit/receive chain between the magnet and the equipment room, the new sold-state RF amplifier system on the side of the magnet, and the fact that BOLD imaging would use a lower % of the maximum gradient strength (same gradient strength as used on the Trio, to avoid severe peripheral nerve and possibly cardiac stimulation) might serve to reduce instrumental noise and so increase the time-series SNR (tSNR) that determines the ability to detect BOLD activations.

Initial tests with the standard water phantom bore this expectation out. Using the 32-channel head coil, and the 3 mm / 500-timepoint EPI-stability protocol we run daily for scanner quality assurance, we observed a ~25% increase in tSNR when the protocol was first implemented on the Prisma^{fit}. However, the BOLD scans conducted on the 8 human subjects suggest that physiological noise in humans, at this frequency and field strength, is a great equalizer [11]. Figure 7 summarizes the tSNR results. The 3 mm / TR = 3 sec / no SMS resting state BOLD scans showed no change in average tSNR across the whole brain for the 8 subjects ($p > 0.05$). At higher spatial resolution, there were small gains in tSNR observed with the Prisma^{fit}. The TR = 2 s / SMS 3 protocol showed a ~5% gain in tSNR – although not statistically significant given the number of subjects ($p > 0.05$). The high temporal resolution resting-state BOLD scans (TR = 750 ms / SMS = 8) showed a modest gain of ~20% when averaged across all subjects ($p < 0.001$). However, benefits for resting-state network analysis were minimal, with improved definition of the networks seen in some subjects, but no quantifiable improvement observed in other subjects, or when averaged over all eight subjects. It is possible that certain tasks that yield weak activations may provide better results on the Prisma^{fit} under conditions of high spatial and/or temporal resolution. But for routine BOLD scans as commonly carried out in neuroimaging studies, with a spatial resolution of ~2.5–3 mm and TR of 2–3 sec, the Prisma will provide similar quality BOLD data to the Trio.

However, the new hardware of the Prisma^{fit} led us to re-evaluate what should be baseline acquisition protocols for BOLD scanning for routine use, with respect to either spatial or temporal resolution. The full details of this BOLD optimization is beyond the scope of this article. However, one example warrants brief mention, for it relies on a combination of improvements in the gradient coil and the improved speed of the new reconstruction

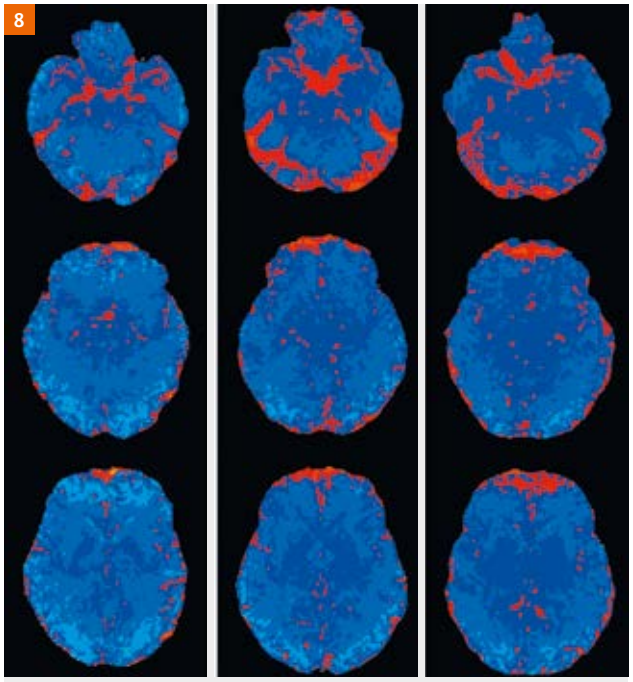

Figure 8:
Maps of tSNR difference in resting-state BOLD scans from three axial slices in three subjects, acquired on the MAGNETOM Prisma^{fit}. Red / orange indicates regions where tSNR is higher using a 1.7 mm resolution / GRAPPA = 2 / SMS = 3 protocol. Blue indicates regions where tSNR is higher with a 2.2 mm / no GRAPPA / SMS = 3 protocol.

computer, combined with simultaneous multi-slice techniques, which allowed us to push the envelope of spatial resolution for whole-brain BOLD scanning beyond what was routinely possible on the Trio, and achieve 1.5 mm and 1.7 mm isotropic resolution that our psychology faculty are now using successfully in standard neuroimaging studies. While not technically impossible on the Trio, the improved slew rate of the Prisma gradient coil and the higher "forbidden echo spacing" range due to acoustic resonances (0.78–0.93 ms vs ~0.58–0.69 ms on the Trio), enable the very large matrix size required for this spatial resolution with only two-fold GRAPPA acceleration to keep the TE to around 30 ms. Along with the improved echo-spacing that makes each echo train slightly shorter, the use of SMS allows the ~80–90 slices required for full brain coverage to be acquired in a 2-second TR, while the improved reconstruction system enables the data to be reconstructed without lagging behind the acquisition, despite the large matrix size and number of slices. Acquiring such data would certainly tax the older reconstruction hardware of the Trio.

The main benefits of using such a high spatial-resolution is to reduce partial volume effects over the cortical surface and to further ameliorate susceptibility-induced dropout and distortion in high-susceptibility areas of the human brain such as the orbital frontal cortex and the temporal poles. In these areas, EPI signal, and BOLD activations, may be seen from brain regions that are often not detected at 3T. (The benefits of higher spatial resolution, while maintaining high MR signal despite using smaller voxels, is one of the benefits of using an ultra-high field MRI system such as the 7T MAGNETOM Terra.) While the tSNR is lower in much of the brain than for acquisition protocols with ~2.0–2.5 mm spatial resolution, on the MAGNETOM Prisma^{fit}, we found the tSNR remained high enough to detect robust BOLD activations such as those of the principal resting-state networks with similar BOLD sensitivity to what was achieved at coarser spatial resolutions. In addition, not only was tSNR improved in the frontal and temporal regions, but we have detected – in numerous subjects – increased tSNR around much of the cortical surface, specifically in visual and parietal regions, where we did not initially expect significant benefit. This improved tSNR at high resolution presumably results from decreased partial-volume effects around the cortical surface, where larger voxels are contaminated by significant amounts of CSF with inherent physiological fluctuations. Figure 8 shows, for 3 axial slices in 3 different subjects, areas in red where tSNR is higher when using a 1.7 mm / TR 2 sec protocol than when using a 2.2 mm / TR 2 sec protocol (2.2 mm being the highest spatial resolution we could achieve without using in-plane acceleration, while keeping TE below 35 ms). The blue regions indicate where the 2.2 mm protocol had higher tSNR, as a result of higher mean signal in the larger voxels. Figure 9 shows group-average functional connectivity maps for 2 different protocols trialed on the Prisma^{fit}, namely the 2.2 mm spatial resolution protocol used in Figure 8 and the 1.5 mm protocol described above. The network maps, from two different seed regions, were remarkably similar despite the reduction in voxel size. Work from some of CBS's psychology faculty users employing the 1.5 mm spatial resolution protocol at 3T is already appearing in the literature [12], while others have employed increased temporal resolution in new studies [13].

Conclusions

The MAGNETOM Prisma^{fit} has been an incredible resource and superb tool for high-quality neuroimaging studies at Harvard's Center for Brain Science Neuroimaging facility. The hardware advances in the MAGNETOM Prisma^{fit}, as compared to the MAGNETOM Trio, provide the potential for significant improvements in diffusion imaging acquisition protocols, while functional (BOLD) imaging can benefit in a narrower range of optimized high-resolution protocols making higher spatial or temporal

9

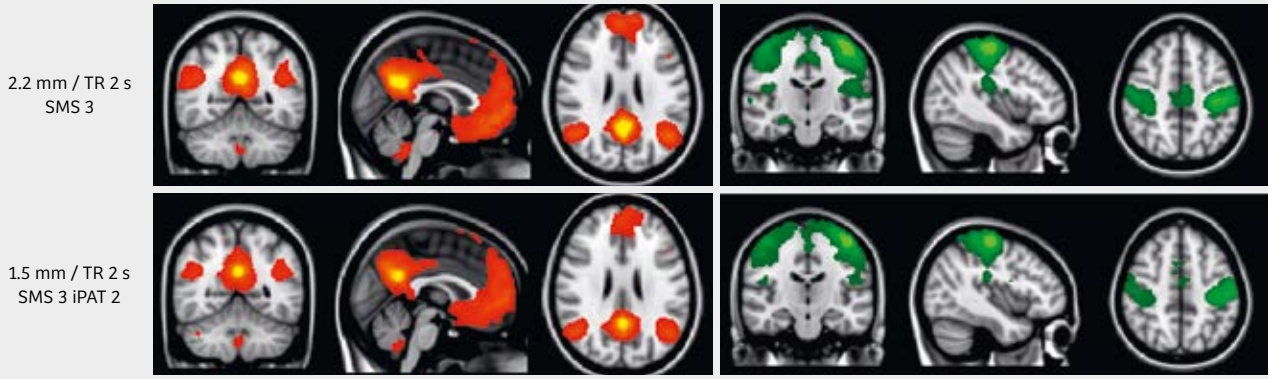

Figure 9:
Group average maps over 8 subjects of two different functional connectivity networks (Default Network from the posterior Cingulate cortex seed, and the Motor network from the left hemisphere Hand region seed) acquired with 2 different acquisition protocols on the MAGNETOM Prisma^{fit}: 2.2 mm / TR 2 sec / SMS = 3, and 1.5 mm / TR 2 sec / iPAT (GRAPPA) = 2 / SMS = 3.

resolution routinely attainable. However, of importance to those running long-term studies that require system stability, we have shown that coarser-resolution BOLD protocols and older, simpler diffusion protocols can be translated from the Trio to the Prisma^{fit} and provide data of a similar quality in terms of signal stability (tSNR), resting state BOLD activation, and standard-deviation of ADC and FA for fixed ROIs of ordered white matter. Additionally, minimal variation is observed in brain morphometric data derived from T1-weighted images from the same subjects, acquired over a 4-month interval, on the Trio and the Prisma^{fit}, indicating that scanner upgrade, in this case, should not bias long-running morphometric studies, provided gradient non-linearity is accounted for.

Acknowledgements

Harvard Center for Brain Science; NIH Shared Instrumentation Grant S10OD020039; NIH Grants P41-RR14075, U24-RR021382.

References

1 van der Kouwe AJ, Benner T, Salat DH, Fischl B. Brain morphometry with multiecho MPRAGE. NeuroImage, 40(2):559–569 (2008).
2 Moeller S, Yacoub E, Olman CA, Auerbach E, Strupp J, Harel N, Uğurbil K. Multiband multislice GE-EPI at 7 Tesla with 16-fold acceleration using Partial Parallel Imaging with application to high spatial and temporal whole-brain fMRI. Magnetic Resonance in Medicine, 63(5);1144–1153 (2010).
3 Setsompop K, Gagoski BA, Polimeni JR, Witzel T, Wedeen VJ, Wald LL. Blipped-controlled aliasing in parallel imaging for simultaneous multislice echo planar imaging with reduced g-factor penalty. Magnetic Resonance in Medicine, 67(5);1210-1224 (2012).
4 Fischl B, Dale AM. Measuring the thickness of the human cerebral cortex from magnetic resonance images. Proceedings of the National Academy of Sciences USA, 97(20):11050-11055 (2000).
5 Reuter M, Rosas HD, Fischl B. Highly Accurate Inverse Consistent Registration: A Robust Approach. NeuroImage, 53(4):1181–1196 (2010).
6 Desikan RS, Segonne F, Fischl B, Quinn BT, Dickerson BC, Blacker D, Buckner RL, Dale AM, Maguire RP, Hyman BT, Albert MS, Killiany RJ. An automated labeling system for subdividing the human cerebral cortex on MRI scans into gyral based regions of interest. NeuroImage, 31(3):968-980 (2006).
7 surfer.nmr.mgh.harvard.edu/fswiki/CorticalParcellation
8 Yeo BT, Krienen FM, Sepulcre J, Sabuncu MR, Lashkari D, Hollinshead M, Roffman JL, Smoller JW, Zöllei L, Polimeni JR, Fischl B, Liu H, Buckner RL. The organization of the human cerebral cortex estimated by intrinsic functional connectivity. Journal of Neuropyhsiology, 106(3);1125-1165 (2011).
9 Mair RW, Reuter M, van der Kouwe AJ. Validation of Cortical Thickness/Volume Data from Multi-Echo MPRAGE Scans with Variable Acceleration in Young and Elderly Populations. Proceedings of ISMRM, 22:1795 (2014).
10 Mair RW, Reuter M, van der Kouwe AJ, Fischl B, Buckner RL. Quantitative Comparison of Morphometric Data from Multi-Echo MPRAGE Variable Acceleration and Different Head Coils. Proceedings of ISMRM, 21:947 (2013).
11 Triantafyllou C, Polimeni JR, Wald LL. Physiological noise and signal-to-noise ratio in fMRI with multi-channel array coils. NeuroImage, 55(2):597-606 (2011).
12 Thakral PP, Benoit RG, Schacter DL. Imagining the future: The core episodic simulation network dissociates as a function of timecourse and the amount of simulated information. Cortex, 90(1):12-30 (2017).
13 Braga RM, Buckner RL. Parallel Interdigitated Distributed Networks within the Individual Estimated by Intrinsic Functional Connectivity. Neuron, 95(1):457–471 (2017).

Contact

Ross W Mair, Ph.D.
Harvard University
Center for Brain Science

NW 231.10
52 Oxford St
Cambridge, MA, 02138
USA
rmair@fas.harvard.edu